Neuro-Oncology

Regulation of bioenergetics through dual inhibition of aldehyde dehydrogenase and mitochondrial complex I suppresses glioblastoma tumorspheres

Junseong Park,[#] Jin-Kyoung Shim,[#] Joon Hee Kang, Junjeong Choi, Jong Hee Chang, Soo-Youl Kim, and Seok-Gu Kang

Department of Neurosurgery, Brain Tumor Center, Severance Hospital, Yonsei University College of Medicine, Seoul, Republic of Korea (J.P., J-K.S., J.H.C., S-G.K.); Cancer Cell and Molecular Biology Branch, Research Institute, National Cancer Center, Goyang, Republic of Korea (J.H.K., S-Y.K.); College of Pharmacy, Yonsei Institute of Pharmaceutical Science, Yonsei University, Incheon, Republic of Korea (J.C.)

Corresponding Authors: Seok-Gu Kang, M.D., Ph.D., Department of Neurosurgery, Brain Tumor Center, Severance Hospital, Yonsei University College of Medicine, 50-1 Yonsei-ro, Seodaemun-gu, Seoul 120-752, Republic of Korea (seokgu9@gmail.com) and Soo-Youl Kim, Ph.D., Cancer Cell and Molecular Biology Branch, Division of Cancer Biology, Research Institute, National Cancer Center, 323 Ilsan-ro, Ilsandong-gu, Goyang 410-769, Republic of Korea (kimsooyoul@gmail.com).

#These authors contributed equally to this work.

Abstract

Background: Targeted approaches for treating glioblastoma (GBM) attempted to date have consistently failed, highlighting the imperative for treatment strategies that operate on different mechanistic principles. Bioenergetics deprivation has emerged as an effective therapeutic approach for various tumors. We have previously found that cancer cells preferentially utilize cytosolic NADH supplied by aldehyde dehydrogenase (ALDH) for ATP production through oxidative phosphorylation (OxPhos). This study is aimed at examining therapeutic responses and underlying mechanisms of dual inhibition of ALDH and OxPhos against GBM.

Methods: For inhibition of ALDH and OxPhos, the corresponding inhibitors, gossypol and phenformin were used. Biological functions, including ATP levels, stemness, invasiveness, and viability, were evaluated in GBM tumorspheres (TSs). Gene expression profiles were analyzed using microarray data. In vivo anticancer efficacy was examined in a mouse orthotopic xenograft model.

Results: Combined treatment of GBM TSs with gossypol and phenformin significantly reduced ATP levels, stemness, invasiveness, and cell viability. Consistently, this therapy substantially decreased expression of genes associated with stemness, mesenchymal transition, and invasion in GBM TSs. Supplementation of ATP using malate abrogated these effects, whereas knockdown of *ALDH1L1* mimicked them, suggesting that disruption of ALDH-mediated ATP production is a key mechanism of this therapeutic combination. In vivo efficacy confirmed remarkable therapeutic responses to combined treatment with gossypol and phenformin.

Conclusion. Our findings suggest that dual inhibition of tumor bioenergetics is a novel and effective strategy for the treatment of GBM.

Keywords

aldehyde dehydrogenase | bioenergetics | glioblastoma | oxidative phosphorylation | tumorsphere

Glioblastoma (GBM), the most common primary brain tumor, continues to be associated with poor prognosis despite the best treatment modalities currently available.[1,2]

One of the major reasons for treatment failure is relapse, which is thought to be attributable, at least in part, to GBM-resident cells with stem cell–like and treatment refractory

Importance of the study

Although GBM is the most common primary brain tumor, the best available treatment options are still associated with poor prognosis owing to the multiplicity of targets and relapse triggered by cancer stemlike cells. Here, we propose a novel therapeutic strategy that targets cancer bioenergetics instead of tumor drivers. We hypothesized that distinct features of GBM metabolism could provide new therapeutic windows that might be expected to overcome previous limitations, including intratumor heterogeneity. In support of this hypothesis, we found that combined treatment with ALDH-targeting gossypol and OxPhos-targeting phenformin significantly reduced ATP levels in GBM TSs, which led to a decrease in stemness, invasiveness, and viability. A preclinical mouse orthotopic xenograft model confirmed these results, definitely demonstrating the in vivo anticancer efficacy of this regimen. We expect that this dual inhibition of bioenergetic pathways could represent a potentially novel therapeutic modality for GBM.

properties, characterized by tumorspheres (TSs) in culture.[3–5] Although numerous targeted therapies have been shown to improve survival of patients with several other types of cancer, no targeted agents superior to Stupp's regimen have been developed for GBM.[2,6] Because of the limited arsenal of clinically applicable drugs and intratumor heterogeneity, an alternative strategy is to target universal features on which GBM primarily depends.[7] Modulation of cancer cell metabolism is one such potential emerging therapeutic strategy.[8,9] Understanding distinct aspects of GBM metabolism may provide an opportunity to develop novel therapeutic approaches for GBM.

The catalytic reaction of aldehyde dehydrogenase (ALDH), which converts aldehyde into carboxylic acid, yields NADH as a by-product. Previous reports have shown that ALDH isoforms are highly upregulated in non–small cell lung cancer (NSCLC).[10,11] We have observed that several ALDH isoforms are also increased in GBM, leading us to hypothesize that GBM metabolism is dependent on ALDH. In this study, we used gossypol to inhibit ALDH activity. Gossypol, a polyphenolic compound commonly extracted from cottonseed, is a pan-ALDH inhibitor that has been tested as an anticancer agent.[10,12] However, treatment with gossypol alone has not proven successful in cancer therapy,[13–15] even though inhibition of the *ALDH1L1* with gossypol has demonstrated effectiveness against NSCLC cell lines and mouse xenograft models.[10] To enhance metabolic disruption in GBM beyond that produced by ALDH inhibition, we further blocked the mitochondrial complex I, the rate-limiting step of the electron transport chain, using phenformin, a biguanide previously used to treat type 2 diabetes.[16,17] In previous reports, several biguanides, including metformin and phenformin, have been proposed as inhibitors of mitochondrial complex I.[17–20] However, the use of phenformin as a standalone treatment for cancer metabolism-based therapy is limited to *LKB1*-deficient tumors[21] and has yielded results that are disappointingly similar to those of treatment with gossypol alone.

Bioenergetics deprivation as a cancer treatment strategy has not been fully explored in the context of GBM. To enhance the efficacy of inhibition of ATP generation in GBM, we utilized combined treatment with gossypol and phenformin, both of which are capable of crossing the blood–brain barrier (BBB).[15] This strategy is predicated on the idea that simultaneous inhibition of multiple bioenergetics pathways would overcome the limitations of either treatment alone. Here, we hypothesized that gossypol and phenformin can induce a profound energy shutdown and subsequent tumor regression in GBM models.

Materials and Methods

Cell Culture and Reagents

Three TS-forming GBM cells were used in this study. GSC11 and TS15-88 are primary tumor cells derived from GBM patients. TS15-88 was established from a fresh GBM tissue specimen, as approved by the institutional review board of the Yonsei University College of Medicine (4-2012-0212, 4-2014-0649). U87 spheres were generated from the U87MG cell line under TS culture condition. For TS culture, cells were cultured in TS complete media composed of Dulbecco's modified Eagle's medium/F12 (Mediatech), 1x B27 (Invitrogen), 20 ng/mL basic fibroblast growth factor, and 20 ng/mL epidermal growth factor (Sigma-Aldrich). All in vitro experiments were performed under TS culture condition. For in vitro treatments, gossypol and phenformin (Sigma-Aldrich) were dissolved in dimethyl sulfoxide (DMSO) and H_2O, respectively, and used at 10 μM. For in vivo studies, gossypol was solubilized in DMSO and mixed with the same volume of cremophor (Sigma-Aldrich); phenformin was dissolved in phosphate buffered saline. For knockdown of *ALDH1L1*, cells were transfected with small interfering (si)RNA duplexes for 48 h using Lipofector-EXT (AptaBio).

Characterization of GBM Tumorspheres

TS formation from human GBM specimens followed previous methods.[22] Immunocytochemistry revealed that all 3 GBMTSs were positive for the stemness markers, cluster of differentiation (CD)133 and nestin (Abcam). Neuroglial differentiation was induced in GBM TSs, as evidenced by the expression of glial fibrillary acidic protein (GFAP) (Dako), myelin basic protein (MBP), neuronal nuclei (NeuN), and tubulin beta 3 (TUBB3) (Chemicon), although GFAP and MBP were not detectable in U87. All 3 GBM TSs successfully generated tumor masses in a mouse orthotopic xenograft model (Supplementary Figure S1).

Gene Expression Microarray Datasets and Analysis

We used datasets curated from the public microarray databases, Gene Expression Omnibus (GEO; n = 245 and n = 401 for normal brain and GBM, respectively)[23] and The Cancer Genome Atlas (TCGA; n = 528). For microarray experiments (Yonsei), total RNA was extracted from GBM TSs using a Qiagen RNeasy Plus Mini Kit and loaded on the Illumina HumanHT-12 v4 Expression BeadChip. Data were variance stabilizing transformed and quantile normalized using the R/Bioconductor lumi package.[24] Expression levels were depicted as heatmaps using GENE-E software. A mitochondrial complex I–related gene list was retrieved from the HUGO Gene Nomenclature Committee database. Functional annotation of differentially expressed genes (DEGs) was performed by overrepresentation analysis using gene sets obtained from MSigDB and QuickGO databases.

Evaluation of ATP, NADH/NAD+ Levels, and Viability

Dispersed GBM TSs were seeded in 96-well plates at a density of 10^4 cells/well. ATP levels were quantified using a CellTiter-Glo luminescent cell viability assay kit (Promega). NADH/NAD+ ratios were determined using a NAD/NADH quantitation colorimetric kit (BioVision). Cell viability was determined by 3 methods: for experiments using malate, a water-soluble tetrazolium salt assay using EZ-Cytox reagent (DoGenBio); for experiments after knockdown, sulforhodamine B assays (Sigma-Aldrich); for others, assay by MTS (3-(4,5-dimethylthiazol-2-yl)-5-(3-carboxymethoxyphenyl)-2-(4-sulfophenyl)-2H-tetrazolium) (Promega).

Sphere Formation Assay

Dissociated 10 single GBM TSs were seeded in 96-well plates and cultured for 3 weeks with TS complete media. TS complete media was supplemented every week. Images were captured and analyzed using ToupView software (ToupTek Photonics).

Invasion Assay

Two-dimensional invasion assays were performed using 24-transwell plates (8-μm pore; Corning). The bottom side of the upper chamber was coated with 0.2% gelatin, and the top side was coated with Matrigel (BD Biosciences) matrix (300 μg/mL). Each upper chamber was seeded with dispersed GBM TSs (5×10^4 cells) supplemented with media without additional growth factors. Then, 500 μL of TS complete media was added to each lower chamber. After 48 h incubation, cells in the upper chamber were paraformaldehyde fixed and stained with crystal violet (Sigma-Aldrich). The Matrigel matrix and remaining cells were removed with cotton swabs, and then images were captured. For 3D invasion assays, each well of a 96-well plate was filled with mixed matrix composed of Matrigel, collagen type I (Corning), and TS complete media. Single spheroids were seeded inside the matrix prior to gelation. Then, TS complete media was added over the gelled matrix to prevent drying. The invaded area was quantified as an occupied area at (72 h–0 h)/0 h.

Flow Cytometry

Expression levels of cell surface markers were evaluated by flow cytometry using antibodies specific for podoplanin (PDPN) (eBioscience) and N-cadherin (R&D Systems). The PDPN primary antibody was directly conjugated with phycoerythrin; N-cadherin was detected using an Alexa Fluor 546–conjugated secondary antibody (Invitrogen). The stained cells were analyzed using an LSR II flow cytometer (BD Biosciences).

Western Blot Analysis

Cell lysates were separated by sodium dodecyl sulfate–polyacrylamide gel electrophoresis on 10% Tris-glycine gels. Proteins were transferred to nitrocellulose membranes and probed with antibodies against ALDH1L1 (Abcam); CD133 and sex determining region Y–box 2 (Sox2) (Merck Millipore); nestin (Novus Biologicals); PDPN, β-catenin, and Snail (Cell Signaling Technology); N-cadherin (R&D Systems); Zeb1 and β-actin (Sigma-Aldrich); Twist, Oct3/4, and glyceraldehyde 3-phosphate dehydrogenase (Santa Cruz Biotechnology). Proteins were detected using horseradish peroxidase–conjugated immunoglobulin G (Santa Cruz Biotechnology), in conjunction with Western Lightning Plus–enhanced chemiluminescence reagent (PerkinElmer). Images were captured using an ImageQuant LAS 4000 mini (GE Healthcare Life Sciences).

Mouse Orthotopic Xenograft Model

Male, 6- to 8-week-old athymic nude mice (Central Lab Animal) were used in this study. All experimental procedures were approved by the Yonsei University College of Medicine Institutional Animal Care and Use Committee. Dissociated U87-luc or GSC11-luc TSs (2×10^5) were implanted into the right frontal lobe of mice at a depth of 4.5 mm using a guide-screw system[25] and Hamilton syringe. Gossypol (40 mg/kg) and phenformin (100 mg/kg) were orally administered daily. If body weight decreased by more than 15% compared with the maximum, mice were euthanized according to the approved protocol, and their brains were removed. For immunohistochemistry, 5-μm-thick sections were obtained with a microtome and transferred onto adhesive slides. Antigen retrieval and antibody attachment were performed using an automated instrument (Discovery XT, Ventana Medical Systems). Zeb1 was detected using an ultraView Universal Alkaline Phosphatase Red Detection Kit (Ventana). CD133, Sox2, N-cadherin, and β-catenin were detected using a peroxidase/3,3′-diaminobenzidine staining system.

Bioluminescence Imaging

Bioluminescence acquisition and analyses were performed using an IVIS imaging system and Living Image v4.2 software (Caliper Life Sciences). Mice were injected intraperitoneally with 100 μL D-luciferin (30 mg/mL; Promega) 15 min prior to signal acquisition, conducted under 2.5% isoflurane anesthesia.

Results

Rationale for Bioenergetics Targeted Therapy in GBM Using Gossypol and Phenformin

To justify combined treatment with gossypol and phenformin in GBM, we compared expression levels of target molecules (ALDH and mitochondrial complex I genes) between normal and GBM samples. An analysis of the GEO microarray database revealed that expression levels of several ALDH isoforms were significantly elevated in GBM (Fig. 1A), which were confirmed in our microarray experiments (Yonsei), including those using normal human astrocyte (NHA), TS, and tissue samples—we compared GBM TS with NHA because subsequent experiments were performed using GBM TSs, which are an exact counterpart of NHA (Fig. 1B). An evaluation of the expression levels of mitochondrial complex I genes (Supplementary Figure S2A) showed that a majority of these genes were significantly overexpressed in GBM TS samples, implying active mitochondrial respiration in GBM TSs (Fig. 1C). For direct verification of energy levels in GBM TSs, we compared NADH/NAD+ ratios under adherent (2D) and sphere (3D) culture conditions. All 3 cells showed elevated NADH/NAD+ ratios under sphere culture conditions, suggesting vigorous energy generation by GBM TSs (Fig. 1D). These evidences support the possibility of bioenergetics targeting in GBM using gossypol and phenformin.

Combined Treatment with Gossypol and Phenformin Reduces ATP Levels and Viability

In cytosol, ALDH is known to convert aldehyde to carboxylic acid, with concurrent generation of the high-energy molecule NADH from NAD+. Therefore, inhibition of ALDH might be expected to inhibit conversion of NAD+ to NADH, which is confirmed in Fig. 2A. Correspondingly, we also showed that gossypol treatment significantly decreased ATP levels in GBM TSs, which was further enhanced by combined treatment with phenformin (Fig. 2B). Changes in cell viability followed a pattern consistent with ATP levels, suggesting the efficacy of this therapeutic strategy (Fig. 2C). To elucidate the mechanisms underlying this therapy, we examined genome-wide effects of gossypol and phenformin treatment by performing a transcriptome analysis of U87 spheres using a microarray. Among the 5038 statistically significant genes, 2223 were exclusively perturbed by the combination of gossypol and phenformin; treatment with either agent alone was associated with relatively fewer perturbed genes (Supplementary Figure S2B, C). To select more definitely influenced genes, we further

evaluated genes with $\log_2$(fold change) > 0.5 differences between control and combination groups. We defined DEGs as genes with $P < 0.05$ and $\log_2$(fold change) > 0.5, and indicated them as blue dots in the volcano plot (Fig. 2D). Functional annotation of DEGs revealed enrichment of several modules associated with metabolism, proliferation, stemness, mesenchymal transition, and invasion (Fig. 2E). According to these results, we specifically examined expression patterns of genes of interest. Stemness-related genes were significantly downregulated by gossypol treatment alone or in combination with phenformin. Similarly, expression levels of genes involved in mesenchymal transition and invasion were also decreased (Fig. 2F, G). Representative genes of each function were confirmed at the protein level by flow cytometry. Expression levels of PDPN and N-cadherin proteins showed patterns consistent with their corresponding mRNA levels (Supplementary Figure S3).

Combined Treatment with Gossypol and Phenformin Suppresses Stemness and Invasiveness

We next evaluated the effects of gossypol and phenformin treatment on the stemness and invasiveness of GBM TSs in relation to changes in the gene expression profile. Neurosphere formation, which is one of the most distinct phenotypes of GBM TSs, was significantly decreased by gossypol treatment. This anti-stemness effect was significantly enhanced by combined treatment with phenformin. Notably, treatment with 10 μM gossypol completely blocked neurosphere formation in U87 spheres (Fig. 3A, B). Consistent with functional assay results, expression of stemness markers, including CD133, nestin, Sox2, PDPN, and Oct3/4, was considerably reduced by gossypol treatment and its combination with phenformin (Fig. 3C). The invasiveness of GBM TSs was also evaluated using transwell invasion assays. The anti-invasive effect of gossypol at a concentration of 1 μM was significantly augmented by the combination with phenformin in all tested cells. At a high concentration (10 μM), gossypol alone was enough to inhibit invasion of U87 and GSC11 cells, and combined treatment with phenformin further significantly reduced invasive cells in TS15-88 (Fig. 3D). Expression of mesenchymal transition- and invasion-related markers, including β-catenin, N-cadherin, Snail, Twist, and Zeb1, was also substantially decreased by gossypol treatment and its combination with phenformin (Fig. 3E). These results suggest that gossypol efficiently suppresses the stemness and invasiveness of GBM TSs, which was significantly enhanced by combined treatment with phenformin.

ATP Supplementation by Treatment with Malate Abrogates the Therapeutic Effects

The malate-aspartate shuttle is a biochemical system for translocating electrons produced in the cytosol across the semipermeable mitochondrial inner membrane to the OxPhos complex. To verify involvement of metabolic disruption in the therapeutic effects of gossypol and phenformin, we exogenously supplemented malate and tested
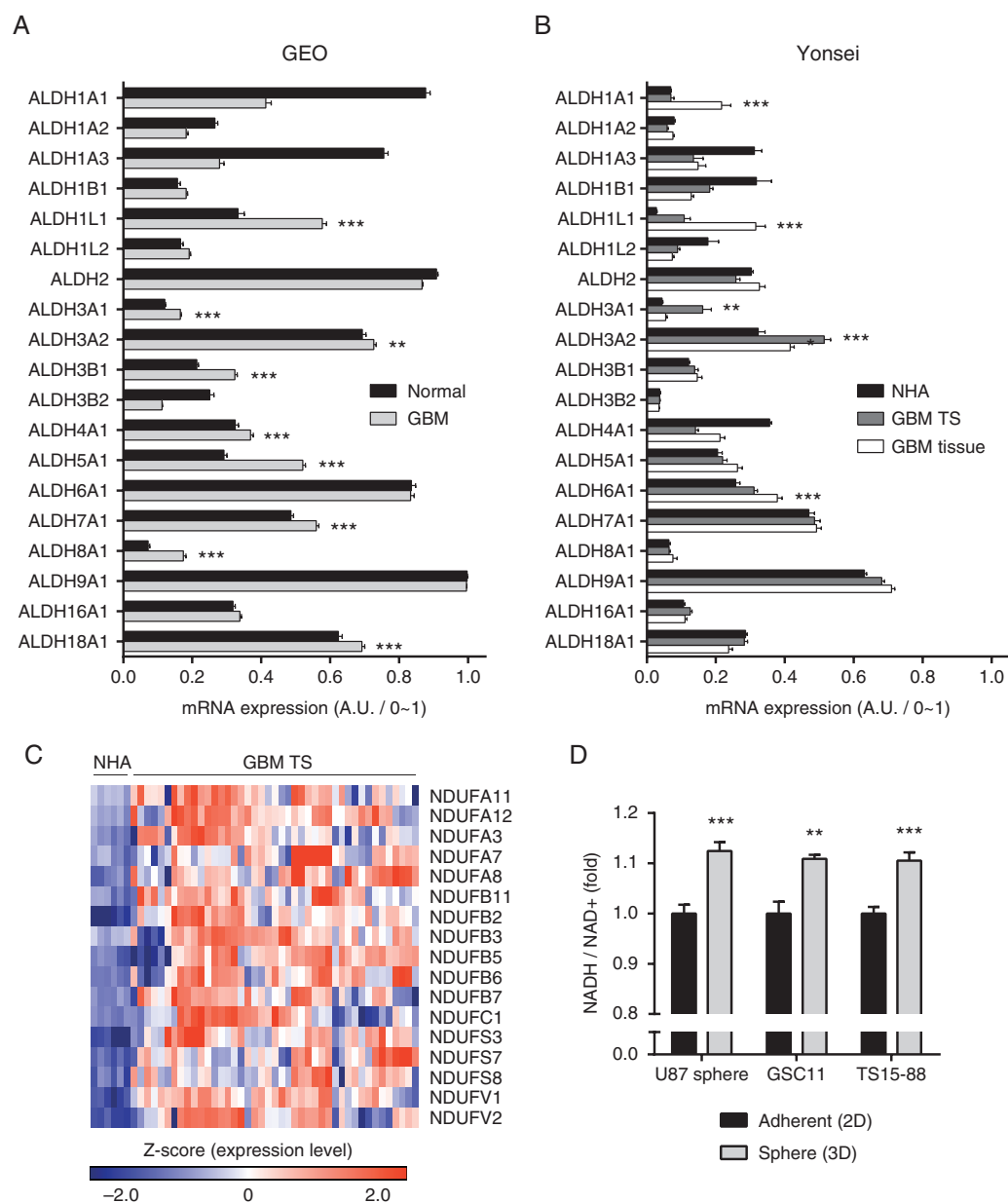
Fig. 1 Metabolic characteristics of GBM. (A, B) Expression levels of ALDH isoforms were evaluated in the GEO microarray database (A) and our microarray data (B) (for Yonsei, NHA, *n* = 6; GBM TS, *n* = 43; GBM tissue, *n* = 38). Means ± SEM; asterisks indicate significantly overexpressed genes (*P < 0.05, **P < 0.01, ***P < 0.001; 2-tailed Student's *t*-test). (C) Expression levels of mitochondrial complex I–related genes were evaluated using the Yonsei microarray dataset. Significantly overexpressed genes are presented as a heatmap. (D) NADH/NAD+ ratio was evaluated for adherent and sphere culture conditions. Means ± SD (**P < 0.01, ***P < 0.001; 2-tailed Student's *t*-test).

whether it can abrogate the efficacy of these drugs. First, we measured ATP levels in U87 spheres after supplementation with malate at different concentrations and durations and confirmed that 48 h treatment with malate significantly increased ATP generation compared with control (Supplementary Figure S4). Under these conditions, malate supplementation significantly abrogated the metabolic disruption, cytotoxicity, and anti-invasion effects of the gossypol and phenformin combination (Fig. 4). These

results suggest that the therapeutic effects of gossypol and phenformin strongly depend on the disruption of bioenergetics.

ALDH Knockdown Mimics the Therapeutic Effects

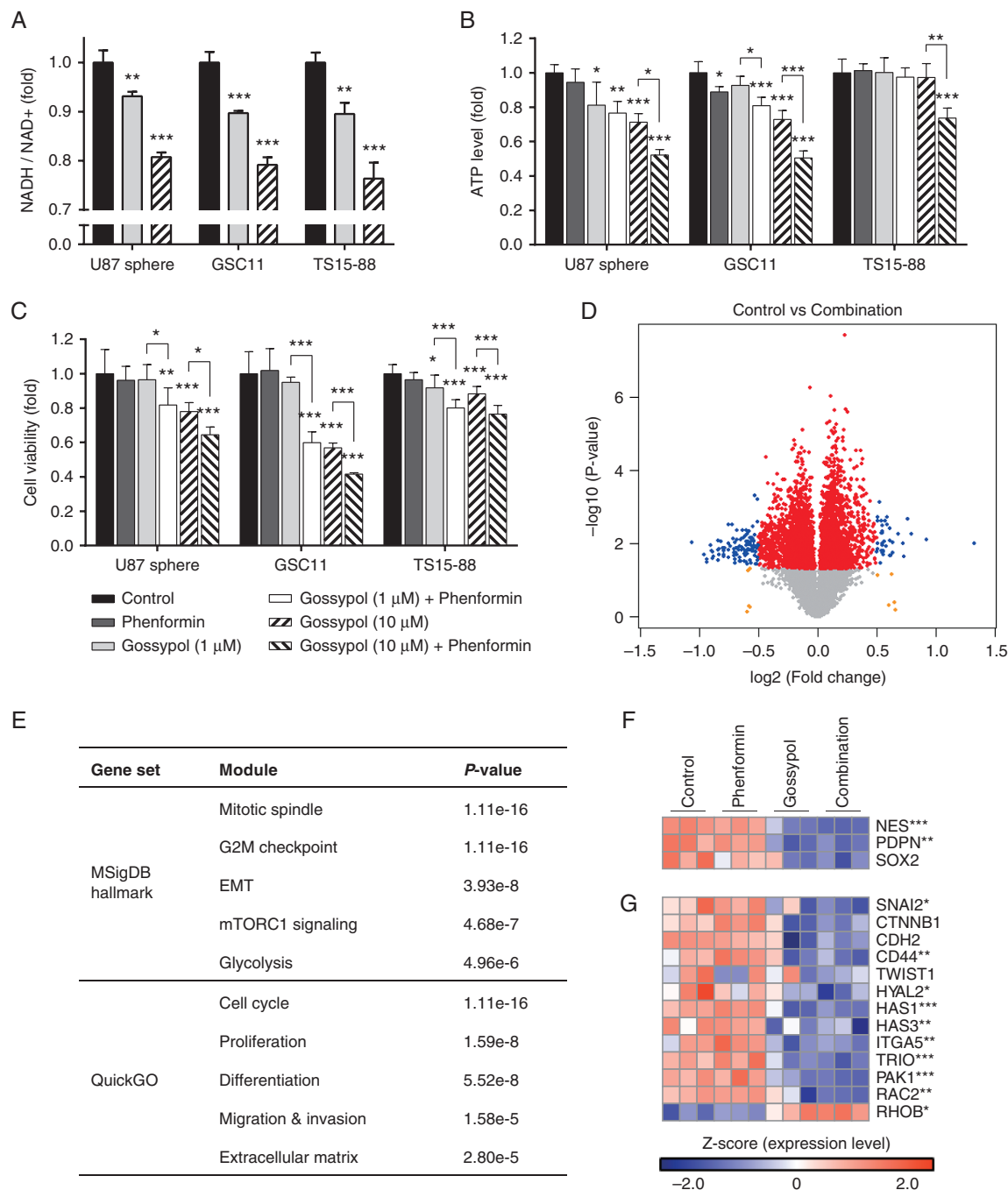The underlying mechanism of gossypol effects on GBM is inferred as inactivation of ALDH and subsequent

Fig. 2 Effects of combined treatment with gossypol and phenformin on GBM TSs. (A–C) NADH/NAD+ ratios, ATP levels, and cell viability were measured 72 h after treatment with gossypol and/or phenformin. Means ± SD; asterisks over the bar denote significant differences compared with controls. (D) U87 spheres were treated with gossypol and phenformin for 72 h, and microarray data were obtained. Volcano plot shows the distribution of genes with differential expression based on *P*-value and fold change. Red, yellow, and blue dots indicate genes with *P*-value < 0.05, $\log_2$(fold change) > 0.5, or both, respectively. (E) Functional annotation of DEGs (blue dots in D) was performed using overrepresentation analysis. Statistical significance was determined using Fisher's exact test, and the top 5 modules are presented. (F, G) Heatmaps displaying expression levels of genes related to stemness (F), mesenchymal transition, and invasion (G). For (A–D), (F), and (G), one-way ANOVA with Tukey's post hoc test (*P < 0.05, **P < 0.01, ***P < 0.001).

reduction in ATP. To confirm mode of actions, we evaluated ATP levels, cell viability, and expression levels of genes related to stemness and mesenchymal transition after

siRNA-mediated knockdown of ALDH, and with the prediction that ALDH knockdown would mimic gossypol therapy. Previous reports on NSCLC,[10] together with expression
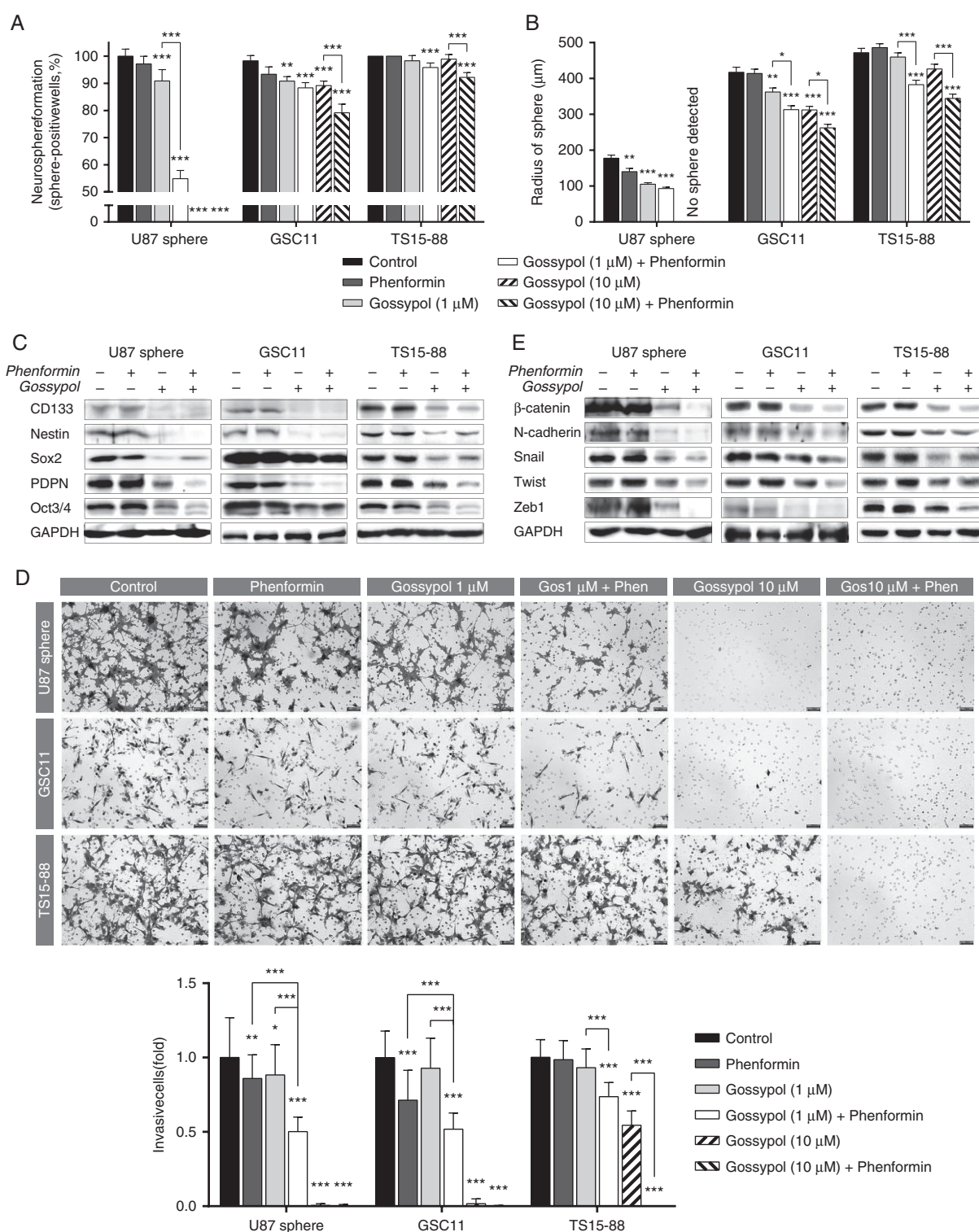
Fig. 3 Evaluation of stemness and invasiveness after treatment with gossypol and phenformin. Stemness and invasiveness were measured 72 h after treatment with gossypol and phenformin. (A, B) Stemness was determined by neurosphere formation assays and quantified as the percentage of sphere-positive wells (A) and sphere radius (B). (C) Expression of stemness-associated genes was measured by western blot. (D) Invasiveness was determined by transwell-based invasion assays. Thirty images were captured per group and invading cells were counted (scale bar = 50 μm). (E) Expression of genes related to mesenchymal transition and invasion was measured by western blot analysis. Differences among groups in (A), (B), and (D) were compared by one-way ANOVA with Tukey's post hoc test; means ± SD; $*P < 0.05$, $**P < 0.01$, $***P < 0.001$, where asterisks denote significant differences between the indicated groups or compared with controls (asterisks over the bar).
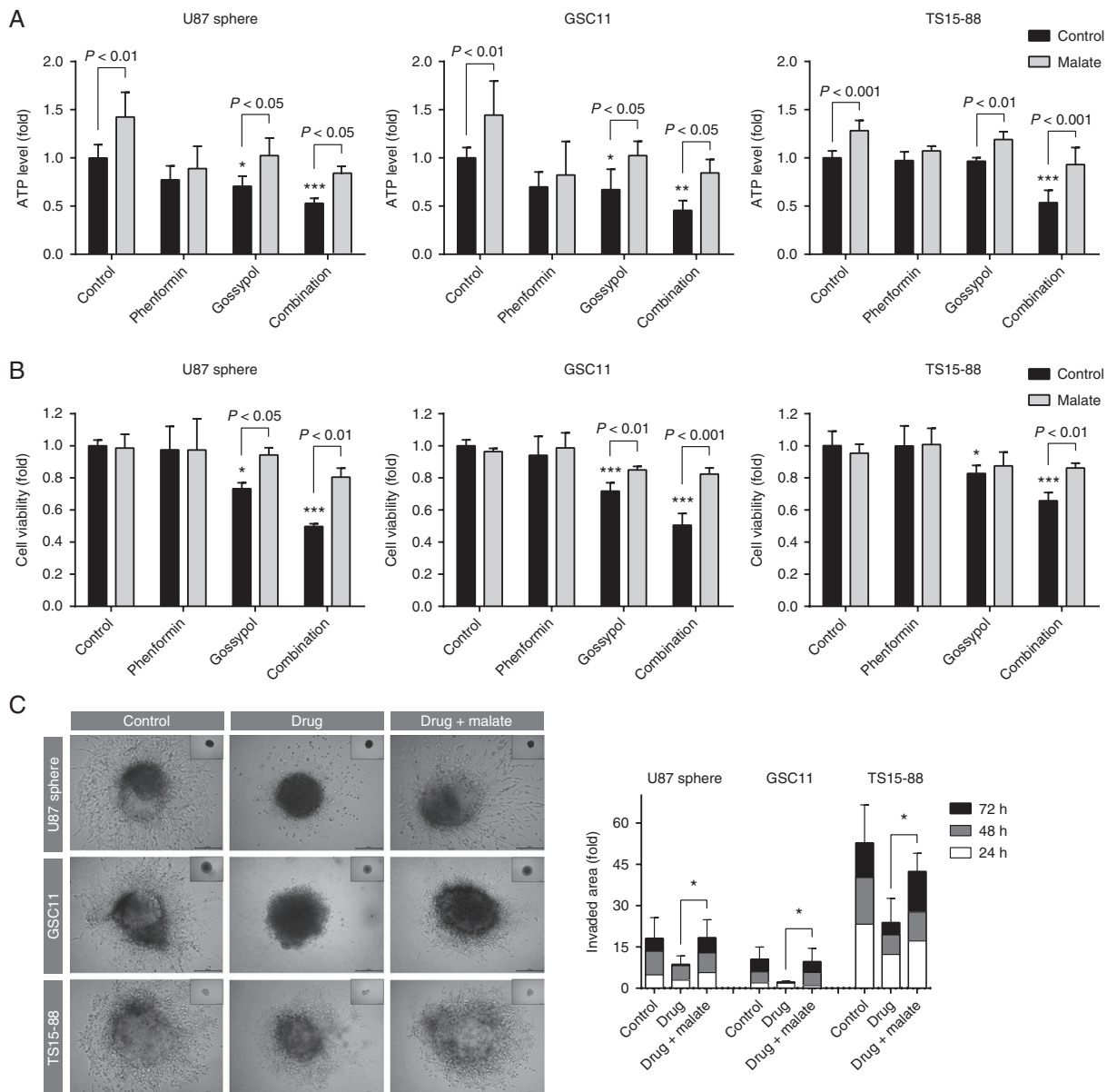
Fig. 4 Malate treatment abolishes the therapeutic effects of gossypol and phenformin. (A, B) ATP levels (A) and cell viability (B) were quantified 72 h after treatment with gossypol and phenformin in the presence or absence of 10 mM malate, added 24 h after drug treatment. One-way ANOVA with Tukey's post hoc test was performed for control groups (black bar). Asterisks indicate significant differences compared with untreated controls (*$P < 0.05$, **$P < 0.01$, ***$P < 0.001$). Control and malate groups were compared by 2-tailed Student's t-test; means ± SD. (C) Invasiveness was evaluated by 3D invasion assay under the same conditions as used for (A, B). Inset photos indicate initial TSs after seeding (0 h). One-way ANOVA with Tukey's post hoc test (means ± SD; *$P < 0.05$, ***$P < 0.001$).

profile data for each ALDH isoform from the GEO, Yonsei (Fig. 1A, B), and National Cancer Institute databases, suggest that *ALDH1L1* is likely responsible for GBM bioenergetics. Consistent with this presumption, knockdown of *ALDH1L1* significantly reduced ATP levels and viability of GBM TSs, mimicking gossypol treatment. Notably, malate supplementation restored *ALDH1L1* knockdown-induced decreases in ATP levels and viability (Fig. 5A, B).

Expression of stemness-, mesenchymal transition-, and invasion-related genes was also considerably diminished by knockdown of *ALDH1L1* (Fig. 5C), suggesting the involvement of ALDH in the mechanism of gossypol and phenformin actions. The expression level of *ALDH1L1* also showed prognostic power in GBM patients. An analysis of GEO and TCGA databases revealed that GBM patients with low levels of *ALDH1L1* showed more favorable prognosis,
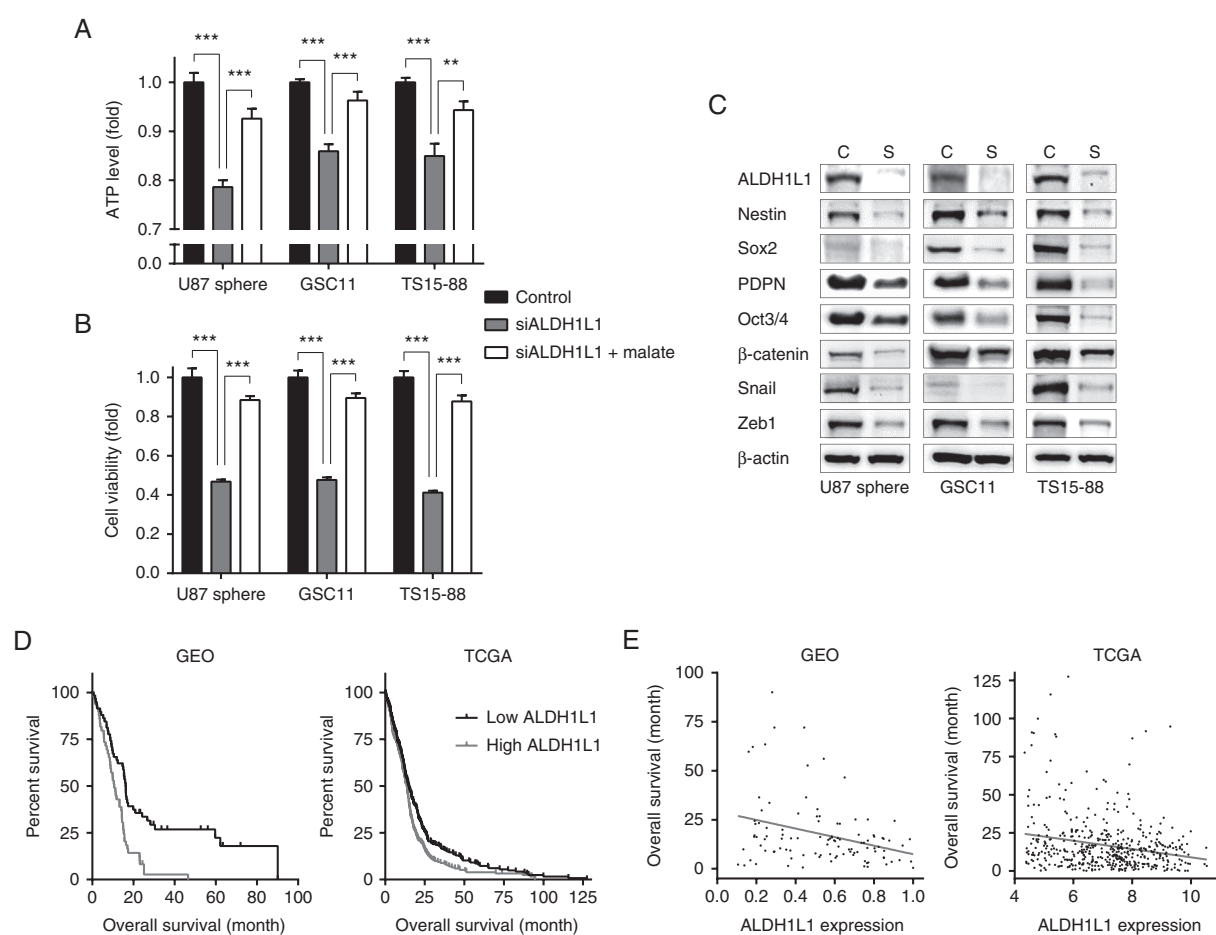
Fig. 5   ALDH knockdown mimics drug treatment. (A, B) Forty-eight hours after transfection with siALDH1L1, ATP levels (A) and cell viability (B) were measured in the presence or absence of 10 mM malate, added 24 h after siRNA transfection (means ± SD; ***$P < 0.001$; 2-tailed Student's t-test). (C) Levels of proteins related to stemness, mesenchymal transition, and invasion were measured by western blot. C indicates control group; S indicates siALDH1L1 group. (D) The entire GBM datasets from GEO and TCGA were divided into 2 groups according to the expression level of *ALDH1L1*. The grouped dataset was subjected to Kaplan–Meier survival analysis to compare overall survival ($P < 0.001$ for GEO and $P < 0.01$ for TCGA; log-rank test). (E) Scatterplot shows the correlation between overall survival of GBM patients and their expression level of *ALDH1L1*. The Pearson correlation was statistically significant ($P < 0.001$, $R = -0.32$ for GEO and $P < 0.001$, $R = -0.23$ for TCGA; the linear regression line is shown.

and *ALDH1L1* expression was negatively correlated with overall survival (Fig. 5D, E), implying positive indications for the use of these therapeutics.

Therapeutic Responses in a Mouse Orthotopic Xenograft Model

The in vivo therapeutic effects of gossypol, with or without phenformin, on tumor growth were investigated in a mouse orthotopic xenograft model using U87-luc cells. Bioluminescence imaging revealed that the rapid tumor growth evident in the untreated group was significantly decreased by combined treatment with gossypol and phenformin, whereas treatment with either gossypol or phenformin alone did not produce a definite regression of tumor mass (Fig. 6A, B). A Kaplan–Meier survival analysis

showed that treatment with gossypol or phenformin alone provided mild survival benefits compared with controls, and combination therapy further prolonged the survival of mice (Fig. 6C). These results were confirmed using a GSC11-based orthotopic xenograft model (Supplementary Figure S5). To quantify invasiveness, we also immunostained for Zeb1 in brain tissue obtained from mice at the end of the experiments. The number of Zeb1+ cells infiltrating outside the gross tumor mass, indicating invading cells, was significantly decreased by the treatments (Fig. 6D). Captured images also showed smoother surfaces at the tumor margin in treated groups. Expression of CD133 and Sox2 (stemness markers) and N-cadherin and β-catenin (mesenchymal transition and invasion markers) was also downregulated by gossypol and phenformin treatment (Fig. 6E). Collectively, these observations clearly demonstrate the in vivo anticancer efficacy of this regimen.
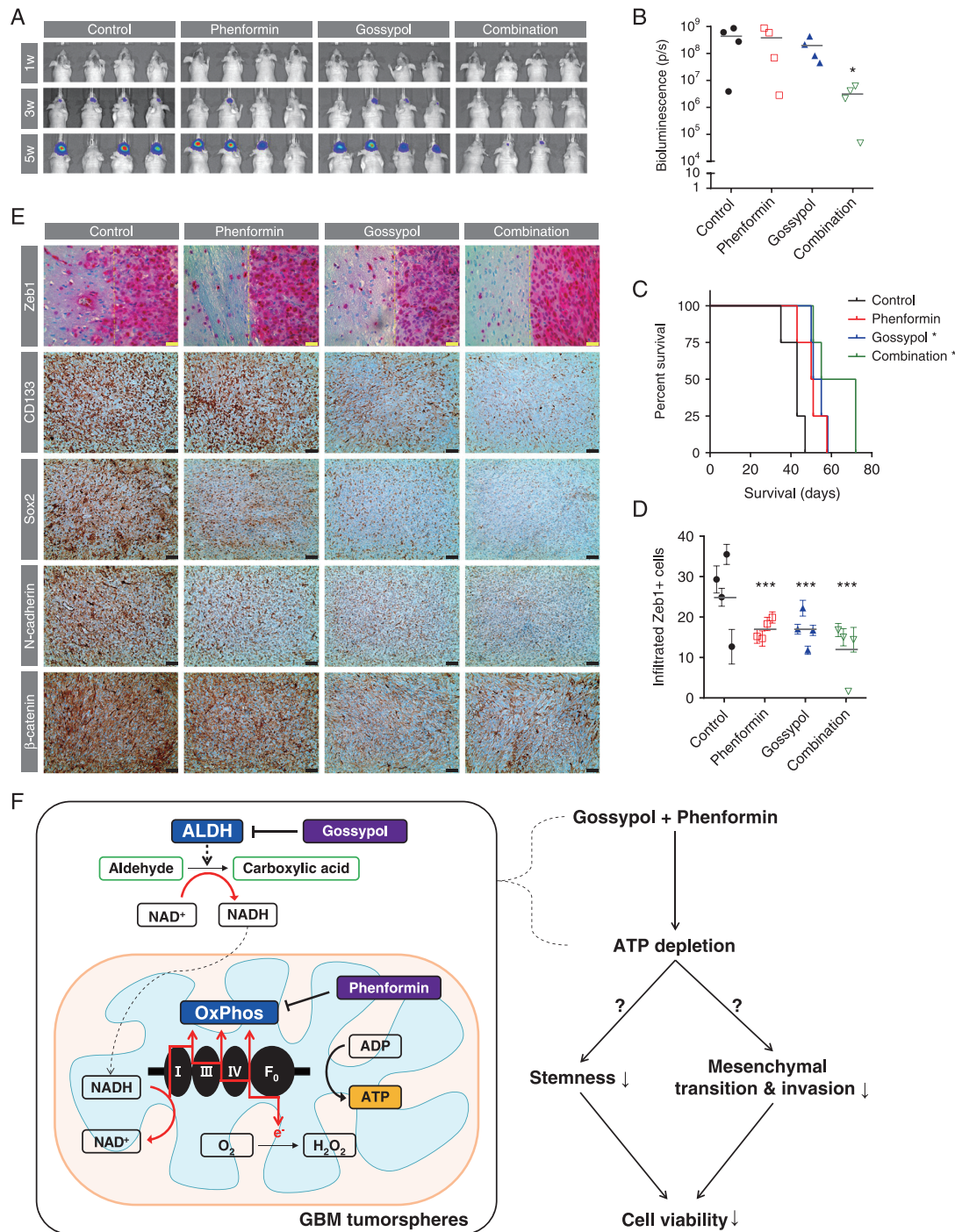
Fig. 6 Therapeutic responses in a mouse orthotopic xenograft model. (A, B) Tumor volume was measured by bioluminescence imaging. Signal intensity was quantified as total photon flux from tissues. One-way ANOVA with Tukey's post hoc test (*P < 0.05). (C) Survival probability for each group was estimated based on Kaplan–Meier curves. Log-rank test (P < 0.001); asterisks indicate groups with significant survival benefits based on Bonferroni-adjusted multiple comparisons (*P < 0.05). (D, E) Sections of the brains obtained from euthanized mice were immunostained for Zeb1 (pink) to identify invading cells (D). The number of infiltrated Zeb1+ cells (left side of yellow line in E), determined from 10 images captured for each mouse, was counted for each group (means ± SEM; ***P < 0.001 compared with controls; 2-way ANOVA with Tukey's post hoc test). Expression levels of CD133, Sox2, N-cadherin, and β-catenin proteins were measured by immunohistochemistry (brown). For all images, hematoxylin (blue) was used to counterstain nuclei (yellow scale bar = 20 μm; black scale bar = 50 μm). (F) Schematic summary of study results. ATP generation by GBM TSs is suppressed by combined treatment with gossypol and phenformin, which target ALDH and OxPhos, respectively. This dual inhibition of tumor bioenergetics attenuates stemness, mesenchymal transition, and invasion, ultimately triggering cell death. Therapeutic responses were confirmed in a preclinical mouse model.

Discussion

Despite recent progress in our understanding of GBM, the prognosis remains grim, including among temozolomide-responsive patients.[1,2] Targeting the stemlike cells in tumor tissue that give rise to GBM TSs in vitro can be a promising solution in that such cells are thought to be major subpopulations responsible for relapse and refractory phenotypes.[3,4] The identification of notable features common to all GBM cells is also required to circumvent intratumor heterogeneity, an important impediment to effective treatment. Against this backdrop, we extensively evaluated the efficacy of cancer bioenergetics regulation as a potential therapy against GBM, using GBM TSs as a model system.

Although the hallmarks of cancer metabolism have been understood for over 90 years,[26] cancer therapeutics targeting bioenergetics have not been established in standard clinical practice. For successful application of metabolism-targeting cancer therapeutics, it is important to understand the distinct dependencies of cancer cells on diverse nutrients as energy sources. Compared with normal cells, cancer cells exhibit enhanced glycolysis, but only a small fraction of the glycolytic flux is transferred to OxPhos.[27] However, OxPhos is still known to be a major supplier of ATP for cancer cells under normoxia,[28,29] implying that these cells can utilize energy sources other than glucose-derived metabolites. In this regard, tracking the source of NADH, a fuel for OxPhos, can provide a clue about cancer-specific metabolic reprogramming. Diverse types of dehydrogenases, including ALDH, can produce NADH, and several ALDH isoforms are potential drug targets because their expression levels are increased in GBM tissues. Notably, ALDH has also been proposed as a stem cell signature in GBM, consistent with our GBM TS model.[30] Our data support that combined treatment with gossypol and phenformin impairs energy generation in GBM TSs, whose bioenergetics depend on ALDH. Although our previous study reported a therapeutic strategy for GBM using combined treatment with 2-deoxyglucose and metformin,[19] we speculated that the combination of gossypol and phenformin would be a superior therapeutic regimen owing to its higher tumor specificity. As shown in Fig. 1, several ALDH isotypes and mitochondrial complex I genes were upregulated in GBM compared with normal. Therefore, our strategy can target distinct metabolic features of GBM, thereby minimizing side effects in normal tissue.

Targeting energy generation in tumor cells using biguanides is an emerging therapeutic strategy in several types of cancers.[17,28] Epidemiological studies have revealed that diabetic patients taking metformin, another type of biguanide, show a significantly reduced risk of tumor incidence,[31] generating increased interest in using metformin as an anticancer agent.[32] However, cellular uptake of metformin, but not phenformin, appears to require the expression of *OCT1*, which is highly expressed in hepatocytes but not elsewhere.[33,34] Moreover, phenformin is a 50-fold more potent inhibitor of mitochondrial complex I than metformin.[18,34] Because of its greater potency and broader tissue availability, phenformin was used here as a combination partner with gossypol to achieve a much greater degree of ATP depletion. Although phenformin has

a higher risk of lactic acidosis compared with metformin (0.4–0.9 and 0.03–0.09 events per 1000 patient-years, respectively),[35] this incidence is a tolerable range compared with several side effects occurring from most anticancer agents.

Here, we examined stemness and invasiveness as remarkable phenotypes of GBM TSs during the progression from ATP reduction to cell death. Since cancer stem cells (CSCs) are known to be responsible for treatment resistance and tumor recurrence,[3,4] inhibitory effects on stemness would be a positive indicator of the potential efficacy of combined treatment with gossypol and phenformin. Moreover, the intrinsic tendency of GBM to infiltrate into normal brain tissue, which is partially mediated by the CSC population,[36] contributes to poor prognosis after surgical resection. Because this combination therapy suppresses invasion, it could be applicable to adjuvant therapy for the potential remaining cancer cells, including CSCs. Therefore, suppression of stemness and invasiveness by our approach is promising and enhances expectations of improved outcome in a clinical setting.

In this study, we showed that combined treatment with gossypol and phenformin induces dual inhibition of bioenergetics by targeting ALDH and OxPhos, causing ATP depletion in GBM TSs. This regimen subsequently attenuated stemness, mesenchymal transition, and invasion, which are prominent features of GBM TSs, ultimately leading to a decrease in cell viability (Fig. 6F). Notably, these results were obtained using patient-derived primary GBM cells and corresponding mouse models, highlighting the clinical applicability of our approach as a novel therapeutic modality for GBM. Moreover, this study offers sufficient flexibility to support combination with established standard treatments. For example, combination with chemotherapy using temozolomide or radiotherapy may further improve the efficacy of our therapy. Future studies will be required to confirm these additional applications.

Supplementary Material

Supplementary material is available at *Neuro-Oncology* online.

References

1. Stupp R, Hegi ME, Mason WP, et al; European Organisation for Research and Treatment of Cancer Brain Tumour and Radiation Oncology Groups; National Cancer Institute of Canada Clinical Trials Group. Effects of radiotherapy with concomitant and adjuvant temozolomide versus radiotherapy alone on survival in glioblastoma in a randomised phase III study: 5-year analysis of the EORTC-NCIC trial. *Lancet Oncol.* 2009;10(5):459–466.

2. Stupp R, Mason WP, van den Bent MJ, et al; European Organisation for Research and Treatment of Cancer Brain Tumor and Radiotherapy Groups; National Cancer Institute of Canada Clinical Trials Group. Radiotherapy plus concomitant and adjuvant temozolomide for glioblastoma. *N Engl J Med.* 2005;352(10):987–996.

3. Jackson M, Hassiotou F, Nowak A. Glioblastoma stem-like cells: at the root of tumor recurrence and a therapeutic target. *Carcinogenesis.* 2015;36(2):177–185.

4. Auffinger B, Spencer D, Pytel P, Ahmed AU, Lesniak MS. The role of glioma stem cells in chemotherapy resistance and glioblastoma multiforme recurrence. *Expert Rev Neurother.* 2015;15(7):741–752.

5. Kang SG, Cheong JH, Huh YM, Kim EH, Kim SH, Chang JH. Potential use of glioblastoma tumorsphere: clinical credentialing. *Arch Pharm Res.* 2015;38(3):402–407.

6. Chinot OL, Wick W, Mason W, et al. Bevacizumab plus radiotherapy-temozolomide for newly diagnosed glioblastoma. *N Engl J Med.* 2014;370(8):709–722.

7. Kim SY. Cancer metabolism: targeting cancer universality. *Arch Pharm Res.* 2015;38(3):299–301.

8. Bobrovnikova-Marjon E, Hurov JB. Targeting metabolic changes in cancer: novel therapeutic approaches. *Annu Rev Med.* 2014;65:157–170.

9. Kim SY. Cancer metabolism: strategic diversion from targeting cancer drivers to targeting cancer suppliers. *Biomol Ther (Seoul).* 2015;23(2):99–109.

10. Kang JH, Lee SH, Lee JS, et al. Aldehyde dehydrogenase inhibition combined with phenformin treatment reversed NSCLC through ATP depletion. *Oncotarget.* 2016;7(31):49397–49410.

11. Kang JH, Lee SH, Hong D, et al. Aldehyde dehydrogenase is used by cancer cells for energy metabolism. *Exp Mol Med.* 2016;48(11):e272.

12. Koppaka V, Thompson DC, Chen Y, et al. Aldehyde dehydrogenase inhibitors: a comprehensive review of the pharmacology, mechanism of action, substrate specificity, and clinical application. *Pharmacol Rev.* 2012;64(3):520–539.

13. Van Poznak C, Seidman AD, Reidenberg MM, et al. Oral gossypol in the treatment of patients with refractory metastatic breast cancer: a phase I/II clinical trial. *Breast Cancer Res Treat.* 2001;66(3):239–248.

14. Ready N, Karaseva NA, Orlov SV, et al. Double-blind, placebo-controlled, randomized phase 2 study of the proapoptotic agent AT-101 plus docetaxel, in second-line non-small cell lung cancer. *J Thorac Oncol.* 2011;6(4):781–785.

15. Bushunow P, Reidenberg MM, Wasenko J, et al. Gossypol treatment of recurrent adult malignant gliomas. *J Neurooncol.* 1999;43(1):79–86.

16. Matsuzaki S, Humphries KM. Selective inhibition of deactivated mitochondrial complex I by biguanides. *Biochemistry.* 2015;54(11):2011–2021.

17. Pollak M. Potential applications for biguanides in oncology. *J Clin Invest.* 2013;123(9):3693–3700.

18. Owen MR, Doran E, Halestrap AP. Evidence that metformin exerts its anti-diabetic effects through inhibition of complex 1 of the mitochondrial respiratory chain. *Biochem J.* 2000;348(Pt 3):607–614.

19. Kim EH, Lee JH, Oh Y, et al. Inhibition of glioblastoma tumorspheres by combined treatment with 2-deoxyglucose and metformin. *Neuro Oncol.* 2017;19(2):197–207.

20. Choi J, Lee JH, Koh I, et al. Inhibiting stemness and invasive properties of glioblastoma tumorsphere by combined treatment with temozolomide and a newly designed biguanide (HL156A). *Oncotarget.* 2016;7(40):65643–65659.

21. Shackelford DB, Abt E, Gerken L, et al. LKB1 inactivation dictates therapeutic response of non-small cell lung cancer to the metabolism drug phenformin. *Cancer Cell.* 2013;23(2):143–158.

22. Kong BH, Park NR, Shim JK, et al. Isolation of glioma cancer stem cells in relation to histological grades in glioma specimens. *Childs Nerv Syst.* 2013;29(2):217–229.

23. Park J, Lee J, Choi C. Evaluation of drug-targetable genes by defining modes of abnormality in gene expression. *Sci Rep.* 2015;5:13576.

24. Du P, Kibbe WA, Lin SM. lumi: a pipeline for processing Illumina microarray. *Bioinformatics.* 2008;24(13):1547–1548.

25. Lal S, Lacroix M, Tofilon P, Fuller GN, Sawaya R, Lang FF. An implantable guide-screw system for brain tumor studies in small animals. *J Neurosurg.* 2000;92(2):326–333.

26. Warburg O, Wind F, Negelein E. The metabolism of tumors in the body. *J Gen Physiol.* 1927;8(6):519–530.

27. Metallo CM, Walther JL, Stephanopoulos G. Evaluation of 13C isotopic tracers for metabolic flux analysis in mammalian cells. *J Biotechnol.* 2009;144(3):167–174.

28. Schulze A, Harris AL. How cancer metabolism is tuned for proliferation and vulnerable to disruption. *Nature.* 2012;491(7424):364–373.

29. Zu XL, Guppy M. Cancer metabolism: facts, fantasy, and fiction. *Biochem Biophys Res Commun.* 2004;313(3):459–465.

30. Nakano I. Stem cell signature in glioblastoma: therapeutic development for a moving target. *J Neurosurg.* 2015;122(2):324–330.

31. Evans JM, Donnelly LA, Emslie-Smith AM, Alessi DR, Morris AD. Metformin and reduced risk of cancer in diabetic patients. *BMJ.* 2005;330(7503):1304–1305.

32. Taubes G. Cancer research. Cancer prevention with a diabetes pill? *Science.* 2012;335(6064):29.

33. Sogame Y, Kitamura A, Yabuki M, Komuro S. A comparison of uptake of metformin and phenformin mediated by hOCT1 in human hepatocytes. *Biopharm Drug Dispos.* 2009;30(8):476–484.

34. Pernicova I, Korbonits M. Metformin—mode of action and clinical implications for diabetes and cancer. *Nat Rev Endocrinol.* 2014;10(3):143–156.

35. Bailey CJ. Metformin: historical overview. *Diabetologia.* 2017;60(9):1566–1576.

36. Ortensi B, Setti M, Osti D, Pelicci G. Cancer stem cell contribution to glioblastoma invasiveness. *Stem Cell Res Ther.* 2013;4(1):18.